PHYSICAL REVIEW B VOLUME 8, NUMBER 5 1 SEPTEMBER 1973

Stopping Power of 1–9-MeV He^{++} Ions in UO_2, (U, Pu)O_2, and ThO_2

V. Nitzki and Hj. Matzke

European Institute for Transuranium Elements, Euratom, D-75 Karlsruhe, Postfach 2266, Germany

(Received 29 December 1972)

The stopping power and the range of He^{++} ions with energies between about 1 and 9 MeV have been measured for the oxides of nuclear interest UO_2, (U, Pu)O_2, and ThO_2, using a new and versatile method. The experimental technique consisted in evaporating oxide layers onto a source emitting α particles of five different energies, and then determining dE/dx by α spectroscopy. These multienergy sources could conveniently be obtained by exposing a metal foil to the recoil atoms of Th^{228}, the radioactive decay chain of which contains five daughter nuclides with different α energies. In addition, the α spectra of thick homogeneous samples were also evaluated and yielded confirmatory results. The data are compared to theoretical calculations. and their application in self-diffusion studies is discussed.

I. INTRODUCTION

Reliable experimental data of the stopping power of elementary particles for a variety of *elements* of intermediate atomic number Z, as well as tables (e.g., Ref. 1) based on the Bethe-Bloch theory of stopping (e.g., Ref. 2) have been published recently. However, predictions for heavy elements and especially compound materials containing heavy elements still involve large errors. This is particularly true for He^{+} ions and α particles, owing partly to the unsatisfactory knowledge of the mean excitation potentials and of the corrections for inner electron shells, and also to the unknown proton-α particle difference. In addition, small ($\lesssim 3\%$) systematic deviations from the Bethe-Bloch prediction can occur.[3]

Consequently, large errors would be expected in any theoretical calculation or semiempirical deduction (e.g., Ref. 4) of the stopping power dE/dx, or the range R, of α particles of low energy (1 to about 6 MeV) in, e.g., uranium and plutonium compounds as was recently demonstrated[5] in a study of dE/dx in UC and (U, Pu)C. These quantities are, moreover, important in certain investigations. For instance, the self-diffusion of uranium and plutonium in UO_2, (U, Pu)O_2, UC, (U, Pu)C, etc., all materials of eminent importance in nuclear technology, is conveniently studied with the aid of the energy loss of the α particles emitted from suitable tracers of uranium and plutonium. In the "α energy degradation method,"[6,7] α spectroscopy is used to deduce depth distributions (and hence diffusion coefficients). Obviously, an exact knowledge of dE/dx is needed for a correct evaluation of the depth distribution from the measured energy distribution.

In addition to values of dE/dx for certain given α energies, the energy dependence of dE/dx must be known if diffusion distances become larger than, say, 1 μm, as is true for any high-temperature studies. Previous self-diffusion studies reported in the literature[8,9] used a calculated dE/dx value only, and completely disregarded the energy dependence of dE/dx. The reported diffusion coefficients can be shown to be in error by $\gtrsim 70\%$. Though a few experimental details on dE/dx in UO_2[10] and PuO_2[11,12] are available in the literature, a more extensive investigation was considered to be necessary. Therefore, the energy dependence of dE/dx of α particles was measured in UO_2, (U, Pu)O_2, and ThO_2 in the energy range of practical interest, i.e., between about 1 and 9 MeV.

II. EXPERIMENTAL

The materials used were high-density reactor-grade UO_2 and $(U_{0.8}Pu_{0.2})O_2$ as well as reagent-grade ThO_2. For energy analysis of the α particles, conventional Si surface-barrier detectors and multichannel analyzers were used. For monoenergetic thin α-emitting sources, Pu^{239} was employed ($E_0 = 5.16$ MeV). For multienergy sources, platelets exposed to a recoil source of Th^{228} were used. Following exposure for a few days, the sources contained the daughter products of Th^{228} [see also Fig. 2(a)], i.e.,

Ra^{224}($E_0 = 5.68$ MeV) ,
Rn^{220}($E_0 = 6.29$ MeV) ,
Po^{216}($E_0 = 6.78$ MeV) ,
Bi^{212}($E_0 = 6.05$ MeV) (only 30% α emission) ,
Po^{212}($E_0 = 8.78$ MeV) .

For the production of thin oxide layers, both conventional high-vacuum-evaporation devices as well as a small electron-beam furnace were used.[13] Thicknesses were determined by weighing, and were varied between 0.1 and 12 μm. X-ray analysis and Rutherford back-scattering techniques were employed to ensure purity of the layers. No impurities were detected. The layers were crystalline

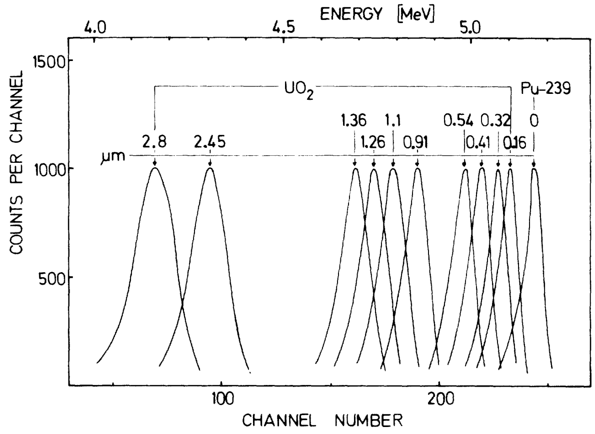

FIG. 1. Energy spectra of a thin source of Pu^{239} before and following evaporation of thin UO_2 layers on top of the source.

and their density was calculated from the measured lattice parameter. The combined error in determining thicknesses (errors in density, size, and weight of the evaporated layers) was $\lesssim 2.5\%$. The error in determining energies was $\lesssim 1\%$.

III. RESULTS

A. Measurements of the Energy Loss dE/dx

Two different techniques were used to measure dE/dx and its energy dependence. These consisted in (1) evaporating successive oxide layers on monoenergetic or multienergy sources and measuring the shift in peak positions or (2) evaluating energy spectra from thick sources.[5]

1. Evaporation of Oxide Layers

In a first set of experiments, successive layers of UO_2 or ThO_2 were evaporated on a monoenergetic source (Pu^{239}, see Fig. 1). The shift of the α line in the energy spectrum was recorded and used to calculate dE/dx.

A much more versatile technique consists in using a multienergy source, e.g., labeled by a Th^{228} recoil source and showing five α lines at different energies [Fig. 2(a)]. If successive oxide layers are evaporated on such sources [Figs. 2(b) and 2(c)], dE/dx values for different energies are obtained for each layer thickness. The layer thickness was increased up to the point that at least some of the α lines could still be separated. The resulting curves, as shown in Fig. 3(a), can be joined together to yield one general curve for each material (both UO_2 and ThO_2), as shown in Fig. 3(b). These curves can be considered to represent the energy loss in layers of up to 25-μm thickness for α particles of the highest energy.

2. Energy Spectra from Thick Sources

As has been demonstrated before[5] for UC and (U, Pu)C, homogeneous thick sources show counting rates which decrease linearly with decreasing energy. Figure 4 shows that this is also the case for (U, Pu)O_2. Here, most of the spectrum is due to the 5.16-MeV α particles of Pu^{239} with only a small contribution of 5.49- and 5.50-MeV α particles of Am^{241} and Pu^{238}, which are present as impurities in technological-grade Pu^{239}. Similar spectra were measured for UO_2.

As demonstrated in Ref. 5, the decrease in counting rate at decreased energies is due to the energy dependence of dE/dx, i.e., to the increase of dE/dx with decreasing energy. Therefore, if influences of energy straggling can be neglected,[14] a relation for dE/dx of the type

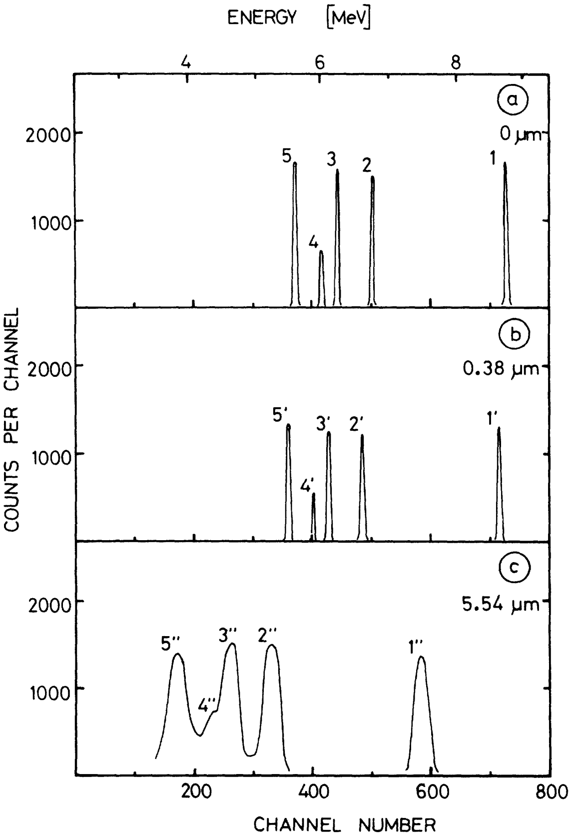

FIG. 2. Energy spectra of a recoil source exposed to a Th^{228} source. The α-radioactive daughters Ra^{224} (5.68 MeV), Rn^{220} (6.29 MeV), Bi^{212} (6.05 MeV), Po^{216} (6.78 MeV), and Po^{212} (8.78 MeV) give rise to five different α lines [part (a)]. Parts (b) and (c) show the shift in energy and the peak broadening due to energy straggling following evaporation of UO_2 layers of 0.38 and 5.54 μm, respectively, on top of the source. The counting times were different for different spectra.

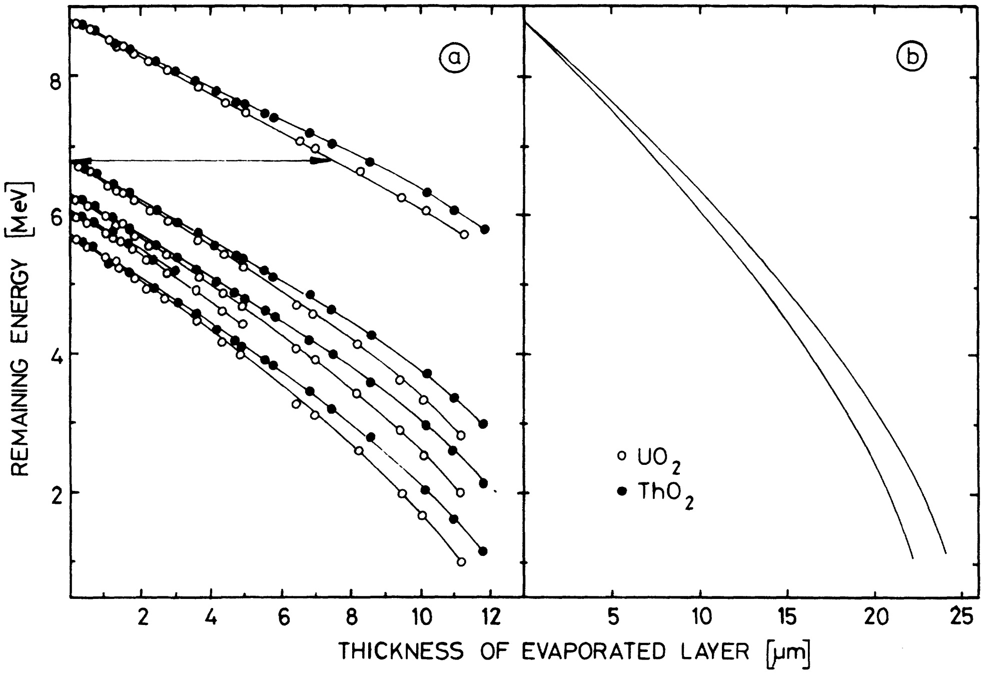

FIG. 3. Part (a) shows the dependence of remaining α-peak energy for the five daughter nuclides of Th^{228}, on the thickness of the evaporated UO_2 and ThO_2 layer, as deduced from spectra as those of Fig. 2. In part (b), the five different curves for each material have been joined together [as indicated by the arrow in part (a)] to yield one curve for each of the two materials, UO_2 and ThO_2.

$$\frac{dE}{dx}=\frac{1}{AE+B}$$

can be deduced from such spectra, thus yielding the complete energy dependence of dE/dx, provided this relation can be normalized with any single value of dE/dx (determined, e.g., as described above in Sec. IIIA1).

The three methods used yielded results which agreed within ±2%; there was no indication of a systematic trend. These combined results are shown in Fig. 5 by the lines labeled "exp" for UO_2, ThO_2, and $(U_{0.8}Pu_{0.2})O_2$. The corresponding mathematical expressions are given in Table I. Note that dE/dx increases with decreasing energy, doubling its value between about 7 and 2 MeV. For comparison, the values are given both in units of keV/μm and of keV/mg/cm^2.

In Table II and Fig. 6 the relation is given between the thickness of the absorbing layer x and the remaining energy E for different original energies E_0 calculated according to the expression

$$x=\int_E^{E_0}\left(\frac{dE}{dx}\right)^{-1}dE\ .$$

Similarly, the range R for any value of E_0 is obtained by setting $E=0$. The results are shown in the insert of Fig. 6, again for the three oxides.

B. Measurement of the Energy Straggling

For all layer thicknesses, the α peaks showed a Gaussian shape, the half-widths of which increased with increasing layer thickness. This is due to statistical fluctuations in the number and kind of collisions along the track of the α particles, which cause unequal energy losses for different particles starting under identical conditions. This effect is

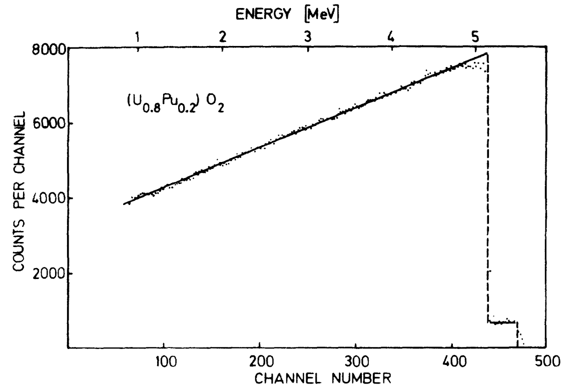

FIG. 4. Energy spectrum of a thick pellet of $(U_{0.8}Pu_{0.2})O_2$ which constitutes a homogeneous and infinitely thick source. Most of the spectrum is due to Pu^{239} (5.16 MeV) with the small extension to 5.50 MeV being caused by Am^{241} and Pu^{238} impurities.

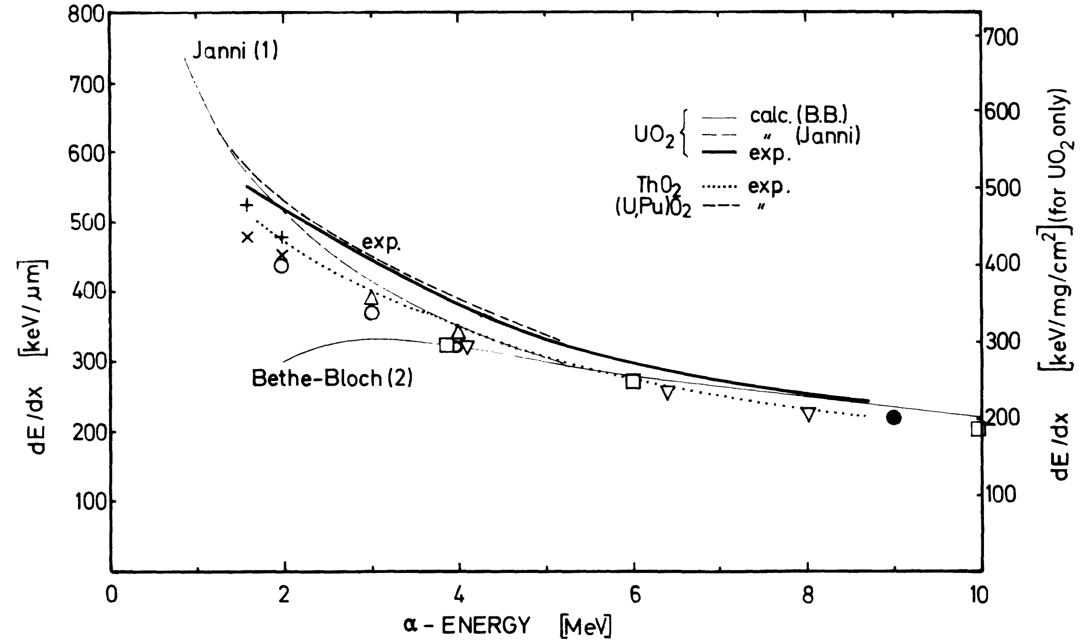

FIG. 5. Differential energy loss dE/dx in keV/μm, for the nuclear oxides ThO_2, UO_2, and $(U_{0.8}Pu_{0.2})O_2$. The thick line for UO_2 and the results for ThO_2 were obtained with evaporated layers; the data for $(U, Pu)O_2$ were deduced from the energy spectrum of a thick pellet. The experimental data for UO_2 are compared with calculated values deduced from the Bethe-Bloch formula (neglecting shell corrections) or from the tables edited by Janni. The scale at the right abscissa in keV/mg/cm² holds for UO_2 only. Included are further experimental data for U and O_2 that have been rearranged for UO_2: +, Bourland, O_2 and Chu, U; × Bourland, O_2 and Northcliffe, U; Δ, Rotondi, O_2 and Chu, U; ○, Rotondi, O_2 and Northcliffe, U; □, Swint, O_2 and Chu, U; ∇, Swint, O_2 and Northcliffe, U; •, Swint, O_2 and Andersen, U.

called "energy or range straggling." As shown in the previous work[5] on UC and (U, Pu)C, the analytical expression for the mean-square deviation $\langle E^2\rangle$ in straggling has the form

$$2\langle E^2\rangle = F_1 x + F_2 ,$$

where x is the thickness of absorbing layer and F_1 and F_2 are constants. The scatter in the data for oxides was worse than that for carbides,[5] but the data followed a similar trend with the constants being

$$F_1 = (145 \pm 40)\times 10^{-4}\ \mathrm{MeV}^2/\mu\mathrm{m} ,$$

$$F_2 = (7 \pm 2)\times 10^{-4}\ \mathrm{MeV}^2 .$$

IV. COMPARISON WITH THEORY

Two theoretical approaches were used for a comparison between theory and experiment. First, dE/dx was calculated according to the Bethe-Bloch formula (e.g. Ref. 2):

$$-\frac{dE}{dx} = \frac{4\pi z^2 e^4}{mv}\,\frac{NZ}{A}\left(\ln\frac{2mv^2}{I} - \frac{C}{Z}\right),$$

where v is the velocity of the α particle, z is the charge of the α particle (i.e., $z = 2$), e and m are the electron charge and mass, N is Avogadro's number, A and Z are the atomic weight and number of the target material, and I is the mean excitation potential. Terms that can be neglected[5] have been omitted. C/Z are so-called shell corrections which compensate for the case that low-energy particles ($E \lesssim 4$ MeV for α particles) have velocities that are no longer large compared to the velocity of the (inner) electrons in their orbitals. For the compound materials considered here, dE/dx is calculated separately for the different elements (hence Z/A) which are weighted by multiplying them with weight factors $W_n = A_n/\sum_\nu A_\nu$. Shell corrections were

TABLE I. Energy dependence[a] of the stopping power of ^4He in ThO_2, UO_2, and $(U, Pu)O_2$.

Material	MeV/μm	MeV/mg/cm²
ThO_2	$\frac{dE}{dx} = \frac{1}{0.348E + 1.46}$	$\frac{dE}{dx} = \frac{1.018}{0.348E + 1.46}$
UO_2	$\frac{dE}{dx} = \frac{1}{0.358E + 1.20}$	$\frac{dE}{dx} = \frac{0.912}{0.358E + 1.20}$
$(U_{0.8}Pu_{0.2})O_2$	$\frac{dE}{dx} = \frac{1}{0.362E + 1.15}$	$\frac{dE}{dx} = \frac{0.904}{0.362E + 1.15}$

[a] Approximate relations describing the curves of Fig. 5. In the energy interval $2 \leq E \leq 8$ MeV, the relations represent the experimental results within better than ± 1%.

TABLE II. Depth-energy relations for ^{4}He in ThO_2, UO_2, and (U, Pu)O_2. x is the depth of emitting atom beneath surface, or thickness of absorbing layer; E_0 is the original energy; and E is the remaining energy following passage through absorbing layer.

Material	μm	mg/cm^2
ThO_2	$x=0.174(E_0^2-E^2)+1.46(E_0-E)$	$x=0.171(E_0^2-E^2)+1.43(E_0-E)$
UO_2	$x=0.179(E_0^2-E^2)+1.20(E_0-E)$	$x=0.196(E_0^2-E^2)+1.32(E_0-E)$
$(U_{0.8}Pu_{0.2})O_2$	$x=0.181(E_0^2-E^2)+1.15(E_0-E)$	$x=0.200(E_0^2-E^2)+1.27(E_0-E)$

not included in these calculations.

One of the calculated curves (for UO_2) is shown in Fig. 5. It describes the experimental data only at high energies (> 8 MeV), whereas at lower energies the experimental results are consistently higher than the calculated ones. For energies below about 3 MeV, the calculated values show the wrong energy dependence, which is due to an increased importance of the neglected shell correction (see also Ref. 5 for this discrepancy and for values of the shell corrections for uranium).

Agreement with theory is better if values taken from the tables provided by Janni[1] for protons and including theoretical shell corrections, are rearranged to yield dE/dx values for α particles. This is shown by the dashed line for UO_2 in Fig. 5 and in Table III, where the Bethe-Bloch results (without C/Z), the results using the Janni tables, and experimental values are given for typical α energies. Table III includes calculated values for U_4O_9 as well. Since Janni did not provide data for Pu, only the Bethe-Bloch and the experimental results are given for the mixed oxide (U, Pu)O_2. Though the calculations according to Janni describe the right energy dependence of dE/dx, there is still a discrepancy as compared to the experimental values of nearly 10%. It seems therefore still to be essential to perform experimental determinations for compound materials containing heavy atoms.

V. COMPARISON WITH LITERATURE DATA

A. General Results on Stopping Power in Gases and Uranium Metal

There are a number of data available on stopping power of protons and/or He^{++} ions in uranium metal and in gases. Typical examples are data of Northcliffe and Schilling[15]: H$^+$ and He^{++} ions in U and O_2, 0 to > 10 MeV; Chu and Powers[16]: He^{++} in U, 0.8–20 MeV; Sørensen and Andersen[17]: H$^+$ in U, 2.25 to > 10 MeV; Rotondi[18]: He^{++} in O_2, 0.1–5.3 MeV; Bourland, Chu, and Powers[19]: He^{++} in O_2, 0.3–2.0 MeV; Swint, Prior, and Ramirez[20]: H$^+$ in O_2, 1.0–3.4 MeV. These data can be rearranged and dE/dx values can be calculated for He^{++} in compounds. As with the data of Janni, various combinations of results were rearranged for UO_2, and plotted in Fig. 5. At higher energies, these results agree with those due to Janni, whereas at lower energies, they tend to be lower by ≈ 10%. The conclusion, therefore, remains that direct experimental determinations for heavy compound materials are essential.

B. Previous Results on UO_2, (U, Pu)O_2, and PuO_2

As mentioned in Sec. I, a few details on the stopping of α particles in UO_2 [10] and (U, Pu)O_2 and PuO_2 [11,12] have been published before. The most extensive study is that for UO_2,[10] where seven successive layers of UO_2 were evaporated on a layer of $(U^{235})O_2(E_0=4.76$ MeV). The range of those

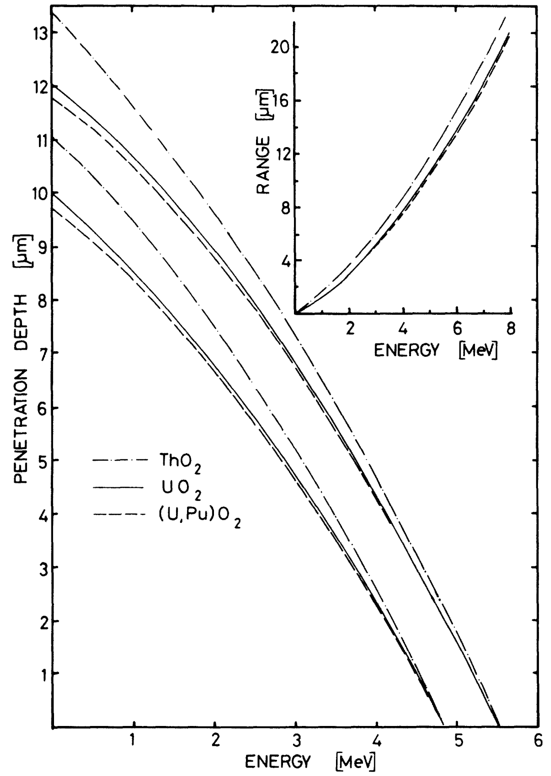

FIG. 6. Range-energy dependence for ThO_2, UO_2, and $(U_{0.8}Pu_{0.2})O_2$ for the two most frequently used tracer nuclides U^{233} (4.82 MeV) and Pu^{238} (5.50 MeV). The insert shows the range of α particles of various energies in the three materials.

TABLE III. Comparison of experimentally determined values of dE/dx (in keV/μm) with calculated ones for three typical α energies.

Energy	UO_2			ThO_2			$(U, Pu)O_2$		U_4O_9	
(MeV)	B. B.[a]	Jan.[b]	Expt.	B. B.	Jan.	Expt.	B. B.	expt.	B. B.	Jan.
4.0	311	355	380	288	332	351	314	385	330	376
4.8	296	319	342	274	298	319	299	346	313	349
5.6	281	291	312	253	262	293	284	314	296	308

[a] B. B. is calculated according to Bethe-Bloch formula (see Ref. 2).

[b] Jan. is rearranged for α particles from tables provided by Janni (see Ref. 1).

α particles was extrapolated to be 10 μm and a dE/dx value of 340 keV/μm for 4.76 MeV can be deduced from the data presented. Given the fact that a comparatively thick source was used in this study (about 0.5-μm thickness), the agreement to the values of the present investigation [for $E = 4.76$ MeV: $R = 9.75$ μm (see Table II and Fig. 6) and $dE/dx = 344$ keV/μm (see Table I and Fig. 5)] can be considered to be excellent.

In the two remaining references (11 and 12), some details on stopping power and range of α particles in $(U, Pu)O_2$ and PuO_2 were deduced from α spectra of thick sources (see Sec. III A 2). In Ref. 11 the molecular stopping cross section $S(E)$ (in eV cm^2/molecule) of α particles in $(U, Pu)O_2$ is given, which can be transformed in energy-loss values (in keV/μm) according to the expression

$$\frac{dE}{dx} = \frac{SN\rho}{M} 10^{-7} ,$$

where N is Avogadro's number, ρ is the density, and M is the molecular weight.

The resulting values, however, were lower (e.g., 324 keV/μm at 4 MeV and 420 keV/μm at 2 MeV) than those reported here, indicating the difficulties of normalizing the results deduced from the spectra, without a separate determination of a single value of dE/dx for a given energy (see also Sec. III A 2 and Ref. 5). Finally, in Ref. 12 the "self-absorption α range" in $(Pu^{238})O_2$ (i.e., the range of 5.5-MeV α particles in PuO_2) was determined to be 11.7 ± 0.2 μm, which is in excellent agreement with the value of 11.8 μm deduced in the present study for $(U, Pu)O_2$ (see Fig. 6 and Table II).

VI. CONCLUSIONS AND SUMMARY

The present investigation extends a previous study[5] on nuclear carbides and provides data for the energy loss and range of α particles for energies between about 1 and 9 MeV for the nuclear oxides UO_2, $(U, Pu)O_2$, and ThO_2. Two techniques already described in Ref. 5 were employed, i.e., evaporation of oxide layers on a thin monoenergetic α source, and evaluation of α spectra of thick samples. For the latter case it was confirmed that the shape of the spectra is inversely proportional to the shape of the energy dependence curve of dE/dx. In addition, a new and more versatile technique was used. This again consisted in evaporating successive oxide layers on an α source which, however, this time was chosen as a thin multienergy source containing five different α energies. Such a source with energies between 5.68 and 8.78 MeV can conveniently be produced by simply exposing for a few days a target disk to a thin layer of Th^{228} acting as recoil source. The decay products are bombarded into the target by the recoil energy of about 100 keV, and their penetration is therefore of the order of 200 Å; hence, the source can be regarded as being thin.

All three techniques yielded results that agreed within ± 2%. The combined results are tabulated. In all cases, the energy dependence of dE/dx can be described by an equation of the type

$$\frac{dE}{dx} = \frac{1}{AE + B} \text{ MeV}/\mu\text{m} \quad (E \text{ in MeV}) .$$

For instance, the equation for UO_2 reads

$$\frac{dE}{dx} = \frac{1}{0.358E + 1.20} \text{ MeV}/\mu\text{m}$$

$$= \frac{0.912}{0.358E + 1.20} \text{ MeV/mg/cm}^2 .$$

The depth-energy relation and the range of α particles in the three oxides were obtained by integration. A typical value, e.g., for 5.5-MeV particles of Pu^{238} in $(U_{0.8}Pu_{0.2})O_2$, is 11.8 μm.

If the experimental results are compared with theoretical calculations using the Bethe-Bloch theory, the expected discrepancy (see, e.g., Ref. 5) is observed if corrections for the inner electron shells are omitted. Especially at low energies, the discrepancies become intolerable ($\gtrsim$ factor of 2). Including shell corrections (e.g., by rearranging the dE/dx values tabulated by Janni[1] for protons and the elements) into the values for α particles and the compounds, decreases the discrepancies which, however, are still $\gtrsim 10\%$. Similar or even larger discrepancies are found if experimental results for protons or helium ions, but for gaseous oxygen and uranium metal, are rearranged to yield data, e.g., for UO_2. The reasons are manifold, and may include deviations from the conventional relationship between $(dE/dx)_p$ and $(dE/dx)_\alpha$ for the heavy elements, the fact that at low energies ($\lesssim 2$ MeV) the α particles can pick up electrons, as well as—for the calculated values—unsatisfactory knowledge of the shell correction term C/Z and the excitation potential I. As an example, for the difficulties encountered while using calculated values, the recent results of Andersen *et al.*[21,22] might be mentioned which indicate an oscillatory dependence between I and the atomic number Z_2 of the target material, whereas normally a smooth variation of I with Z_2 is assumed.

The data presented here are of immediate importance for self-diffusion measurements in the oxides, which conveniently (and by now also conventionally) can be performed with the aid of the α-energy degradation method, i.e., by using α spectroscopy to follow the extension into increasing depths of thin tracer layers which originally had been deposited on the surface of the diffusion specimens.

ACKNOWLEDGMENTS

The authors would like to thank Dr. H. J. Hirsch for experimental help in the early stages of this investigation. One of us (V. N.) would like to thank the Bundesministerium für Wissenschaft und Forschung for financial support.

---

[1] J. F. Janni, Air Force Weapons Laboratory Technical Report No. AWFL-TR-65-150, 1966 (unpublished).

[2] H. A. Bethe, Ann. Phys. (Leipz.) **5**, 325 (1930); F. Bloch, Z. Phys. **81**, 363 (1933).

[3] H. H. Andersen, H. Simonsen, and H. Sørensen, Nucl. Phys. A **125**, 171 (1969).

[4] W. Whaling, in *Handbuch der Physik*, edited by S. Flügge (Springer, Berlin, 1958), Vol. 34, p. 13.

[5] H. J. Hirsch and Hj. Matzke, J. Nucl. Mater. **45**, 29 (1972/73).

[6] F. Schmitz and R. Lindner, J. Nucl. Mater. 17, 259 (1965).

[7] F. Schmitz, Ph.D. thesis (Technical University, Brunswick, 1965) (unpublished).

[8] C. B. Alcock, R. J. Hawkins, A. W. D. Hills, and Ph. McNamara, in *Thermodynamics* (IAEA, Vienna, 1966).

[9] R. J. Hawkins and C. B. Alcock, J. Nucl. Mater. **26**, 122 (1968).

[10] J. F. Marin and M. Coniglio, Nucl. Instrum. Methods **42**, 302 (1966).

[11] J. K. Butler and D. Clarke, J. Nucl. Mater. 33, 208 (1969).

[12] G. N. Huffman and C. J. Kershner, Nucl. Appl. Techn. **9**, 434 (1970).

[13] H. J. Hirsch, Ph.D. thesis (Technical University, Brunswick, 1970) (unpublished).

[14] H. J. Hirsch and Hj. Matzke (unpublished).

[15] L. C. Northcliffe and R. F. Schilling, Nucl. Data A 7, 233 (1970).

[16] W. K. Chu and D. Powers, Phys. Lett. A **38**, 267 (1972).

[17] H. Sørensen and H. H. Andersen, Phys. Rev. B (to be published).

[18] E. Rotondi, Radiat. Res. **33**, 1 (1968).

[19] P. D. Bourland, W. K. Chu, and D. Powers, Phys. Rev. B **3**, 3625 (1971).

[20] J. B. Swint, R. M. Prior, and J. J. Ramirez, Nucl. Instrum. Methods **80**, 134 (1970).

[21] H. H. Andersen, H. Sørensen, and P. Vajda, Phys. Rev. **180**, 373 (1969).

[22] H. H. Andersen, H. Simonsen, H. Sørensen, and P. Vajda, Phys. Rev. **186**, 372 (1969).